Supplementary Information

Bio-based carbonaceous composite materials from epoxidised linseed oil, bio-derived curing agent and starch with controllable functionality

Curing study of the reactive mixtures using FT-IR

The addition of Starbon® scarcely altered the spectra of both reactive mixtures and cured films; however the ester band at 1736 cm^{-1} of the cured control sample showed slightly higher intensity than ones with fillers, suggesting higher degree of crosslinking as confirmed by DSC study.

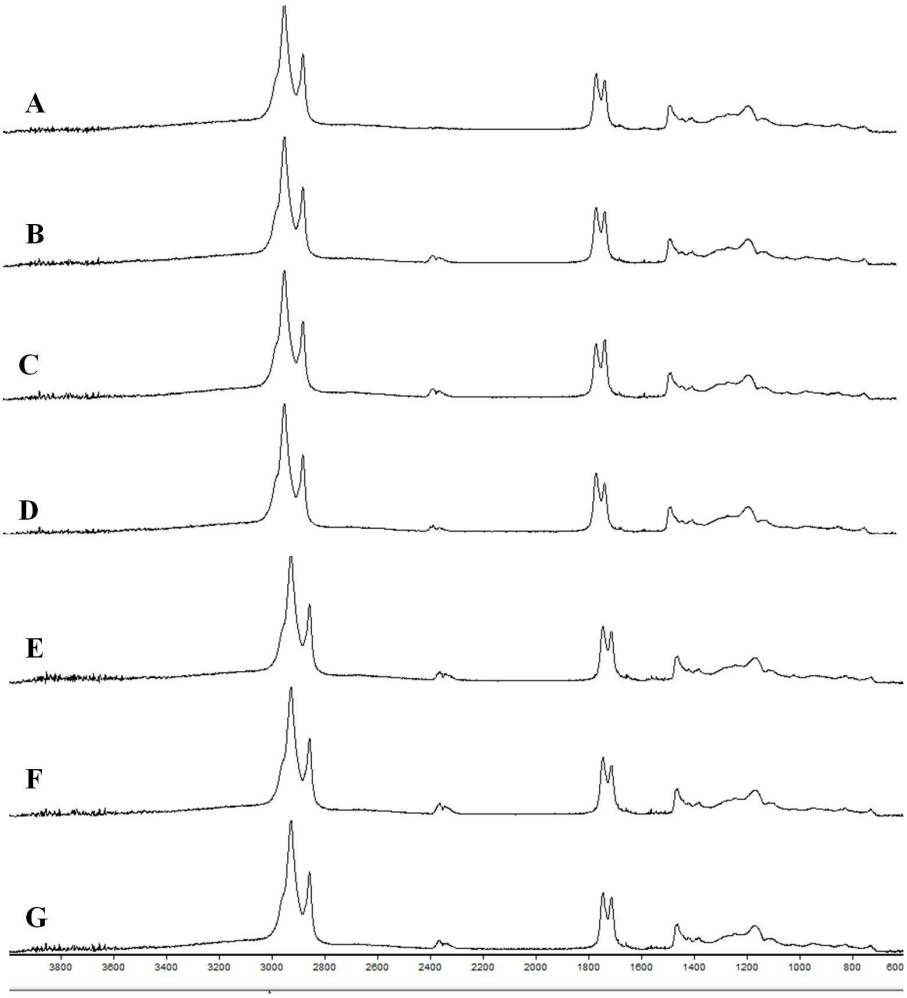

Fig. S1 FT-IR spectra of reactive mixtures (before curing) A. control, B. 5% S300, C. 10% S300, D. 20% S300, E. 5% S800. F. 10% S800, G. 20% S800.

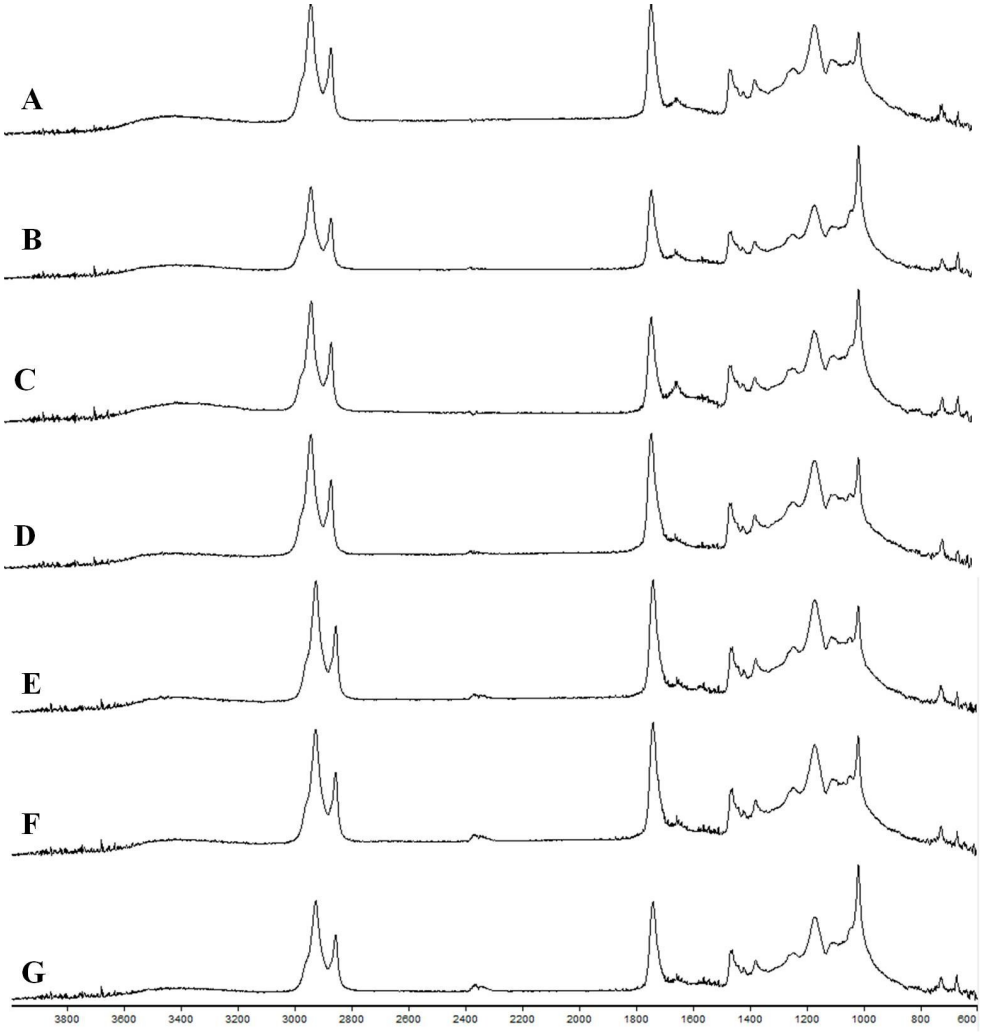

Fig. S2 FT-IR spectra of thermoset films (after curing) A. control, B. 5% S300, C. 10% S300, D. 20% S300, E. 5% S800. F. 10% S800, G. 20% S800.

Thermal analysis of the reactive mixtures

Table S1 summarises the heat of reaction (and heat of reaction normalised, excluding the filler mass), the peak and onset temperatures of the studied reactive mixtures and the glass transitions (T_g) of the cured materials.

Table S1 Summary of MDSC results of reactive mixtures

Formulation	Heat of reaction[a] (J/g)	Normalised heat of reaction (J/g)	Onset temperature[a] (°C)	Peak temperature[a] (°C)	T_g[b] (°C)
Control	151	151	100.6	139.8	-13.7
5%S300	152	160	104.3	142.9	-14.8
10%S300	111	123	114.9	152.3	-15.7
20%S300	115	144	117.4	166.5	-16.4
5%S800	134	141	108.1	144.5	-13.4
10%S800	149	166	101.9	140.7	-13.7
20%S800	122	153	104.4	143.5	-11.0

[a]Non-reversing heat flow (1st heating cycle); [b]Reversing heat flow (2nd heating cycle).

The uniform distribution of Starbon® particles results in single curing transition with no evident sign of post-cure in second heating cycle.

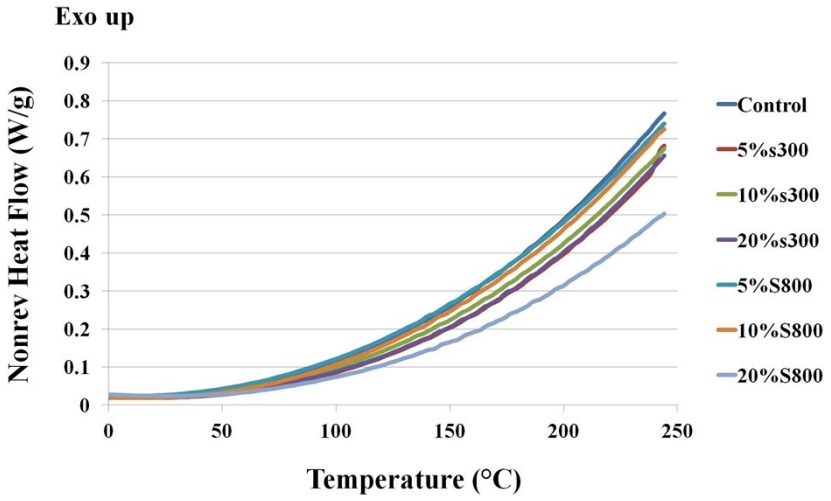

Fig. S3 DSC thermograms of the second heating cycle of formulations comprised of ELO, Pripol, DMAP and different amounts of S300 and S800 (5, 10 and 20%wt.).

Thermal stability of the composites

Table S2 summarises data from TGA measurement of the thermoset composites including the temperature when the original sample weight decreased by 5% ($T_{5\%}$) and by 50% ($T_{50\%}$), residue weight at 550 °C and the maximum temperature of the two-stage thermal decomposition (T_{MAX} 1 and T_{MAX} 2).

Table S2 TGA and dTG results summary of thermoset composites.

Formulation	**$T_{5\%}$ (°C)**	**$T_{50\%}$ (°C)**	**Residual weight at 550 °C (%)**	**T_{MAX} 1 (°C)**	**T_{MAX} 2 (°C)**
Control	362	422	0.9	402	456
5%S300	352	417	4.1	407	455
10%S300	353	429	7.4	402	455
20%S300	348	431	11.7	404	456
5%S800	365	426	4.4	402	456
10%S800	364	431	12.2	405	455
20%S800	365	444	21.8	403	447

Morphological study of the composites

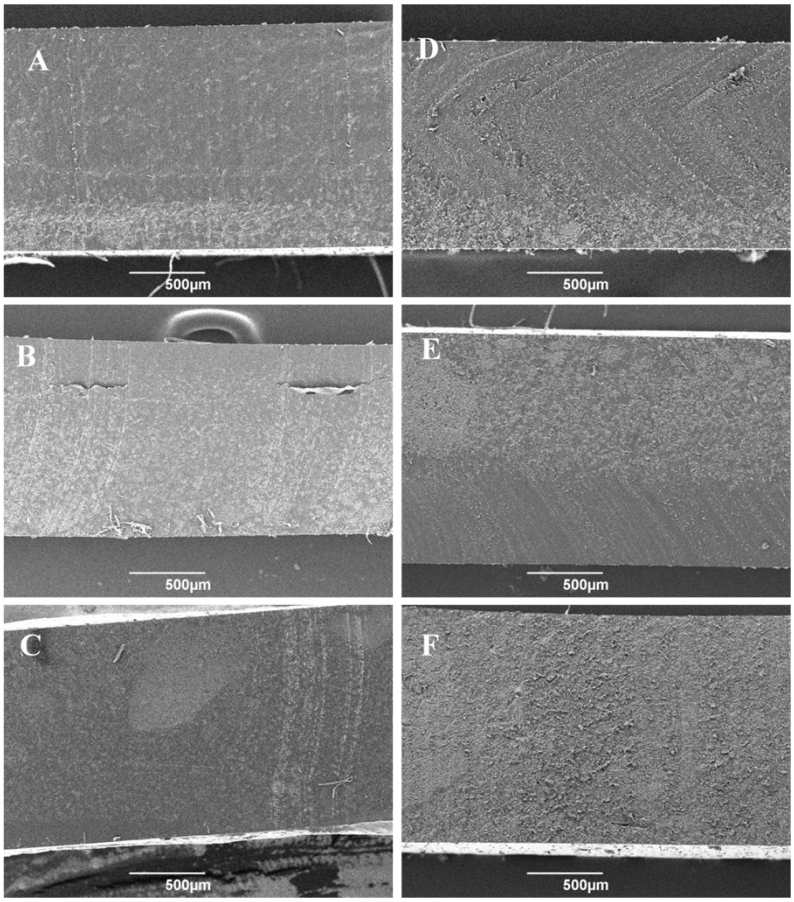

Fig. S4 Scanning electron micrographs of the cross-section of thermoset films with different loading of S300 (A, B, C) and S800 (D, E, F) at 5%, 10% and 20% respectively.

Dynamic mechanical analysis of the composites

Table S3 Storage modulus and T_g of the composites for S300

Temperature (°C)	**Storage modulus (MPa)**			
	Control	**5%S300**	**10%S300**	**20%S300**
-120	5982	4247	3628	4490
-60	3833	3014	2459	3574
-30	3123	2378	2045	3049
-15	1836	1580	1338	1866
T_g *(°C)	-26.0	-21.2	-25.0	-23.5

*: Calculated on the onset of the storage modulus drop.

Table S4 Storage modulus and T_g of the composites for S800

Temperature (°C)	**Storage modulus (MPa)**			
	Control	**5%S800**	**10%S800**	**20%S800**
-120	5982	7040	3504	5217
-60	3833	4724	2376	3856
-20	2432	2980	1593	2763
-10	1003	1160	816	1270
T_g *(°C)	-26.0	-24.9	-20.7	-21.9

*: Calculated on the onset of the storage modulus drop.

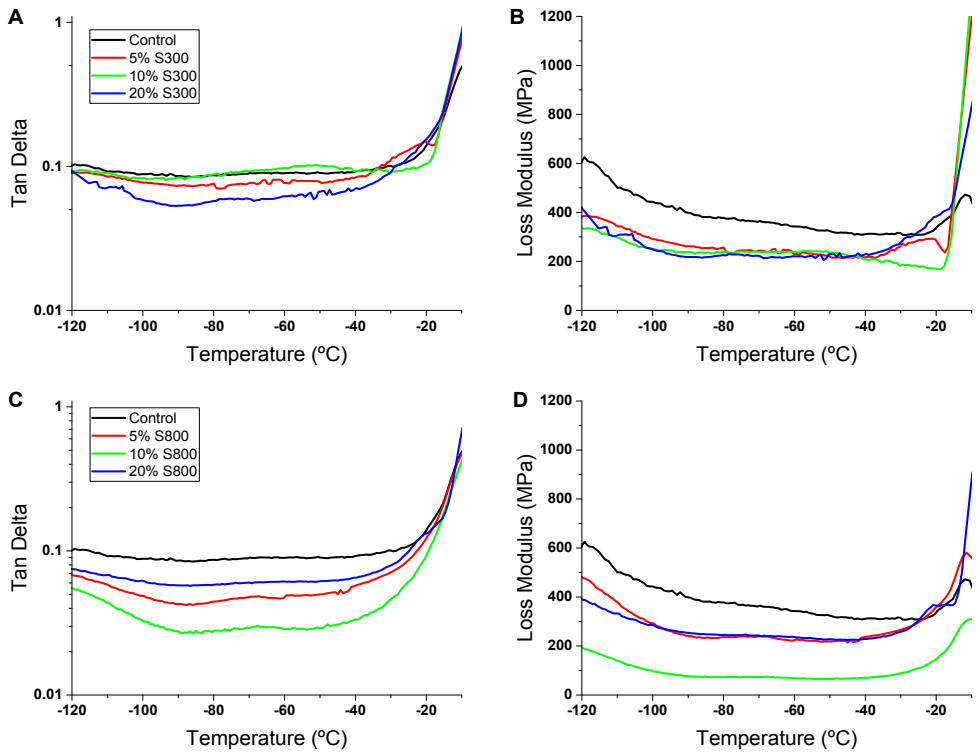

Fig. S5 Tan δ and loss modulus of the composites from DMA analysis - S300 (A and B) and S800 (C and D).